UNIVERSITY OF BIRMINGHAM

University of Birmingham
Research at Birmingham

Understanding the shrinkage of optical absorption edges of nanostructured Cd-Zn sulphide films for photothermal applications

Hossain, Md. Sohrab; Kabir, Humayun; Rahman, M. Mahbubur; Hasan, Kamrul; Bashar, Muhammad Shahriar; Rahman, Mashudur; Gafur, Md. Abdul; Islam, Shariful; Amri, Amun; Jiang, Zhong-tao; Altarawneh, Mohammednoor; Dlugogorski, Bogdan Z.

Link to publication on Research at Birmingham portal

Accepted Manuscript

Title: Understanding the Shrinkage of Optical Absorption Edges of Nanostructured Cd-Zn Sulphide Films for Photothermal Applications

Author: Md. Sohrab Hossain Humayun Kabir M. Mahbubur Rahman Kamrul Hasan Muhammad Shahriar Bashar Mashudur Rahman Md. Abdul Gafur Sariful Islam Amun Amri Zhong-Tao Jiang Mohammednoor Altarawneh Bogdan Z. Dlugogorski

Please cite this article as: Md.Sohrab Hossain, Humayun Kabir, M.Mahbubur Rahman, Kamrul Hasan, Muhammad Shahriar Bashar, Mashudur Rahman, Md.Abdul Gafur, Sariful Islam, Amun Amri, Zhong-Tao Jiang, Mohammednoor Altarawneh, Bogdan Z.Dlugogorski, Understanding the Shrinkage of Optical Absorption Edges of Nanostructured Cd-Zn Sulphide Films for Photothermal Applications, Applied Surface Science http://dx.doi.org/10.1016/j.apsusc.2016.09.095

This is a PDF file of an unedited manuscript that has been accepted for publication. As a service to our customers we are providing this early version of the manuscript. The manuscript will undergo copyediting, typesetting, and review of the resulting proof before it is published in its final form. Please note that during the production process errors may be discovered which could affect the content, and all legal disclaimers that apply to the journal pertain.

Understanding the Shrinkage of Optical Absorption Edges of Nanostructured Cd-Zn Sulphide Films for Photothermal Applications

Md. Sohrab Hossain[a], Humayun Kabir[a,b], M. Mahbubur Rahman[a,c*], Kamrul Hasan[d], Muhammad Shahriar Bashar[e], Mashudur Rahman[e], Md. Abdul Gafur[f], Sariful Islam[g], Amun Amri[h], Zhong-Tao Jiang[c], Mohammednoor Altarawneh[i], Bogdan Z. Dlugogorski[i]

[a]Department of Physics, Jahangirnagar University, Savar, Dhaka 1342, Bangladesh

[b]School of Metallurgy and Materials, University of Birmingham, Edgbaston, Birmingham B15 2TT, United Kingdom

[c]Surface Analysis and Materials Engineering Research Group

School of Engineering & Information Technology, Murdoch University, Perth, Western Australia 6150, Australia

[d]Department of Chemistry, College of Sciences, University of Sharjah, P. O. Box 27272, Sharjah, United Arab Emirates

[e]Institute of Fuel and Research Development, Bangladesh Council for Scientific and Industrial Research, Dhanmondi, Dhaka, Bangladesh

[f]Pilot Plant and Process Development Center, Bangladesh Council for Scientific and Industrial Research, Dhanmondi, Dhaka, Bangladesh

[g]Department of Physics, Comilla University, Comilla, Bangladesh

[h]Department of Chemical Engineering, Universitas Riau, Pekanbaru, Indonesia

[i]School of Engineering & Information Technology, Murdoch University, Murdoch, WA 6150, Australia

***Corresponding Author**: School of Engineering & Information Technology, Murdoch University, Australia. *E-mail address*: M.Rahman@Murdoch.edu.au (M.M. Rahman)

Graphical abstract:
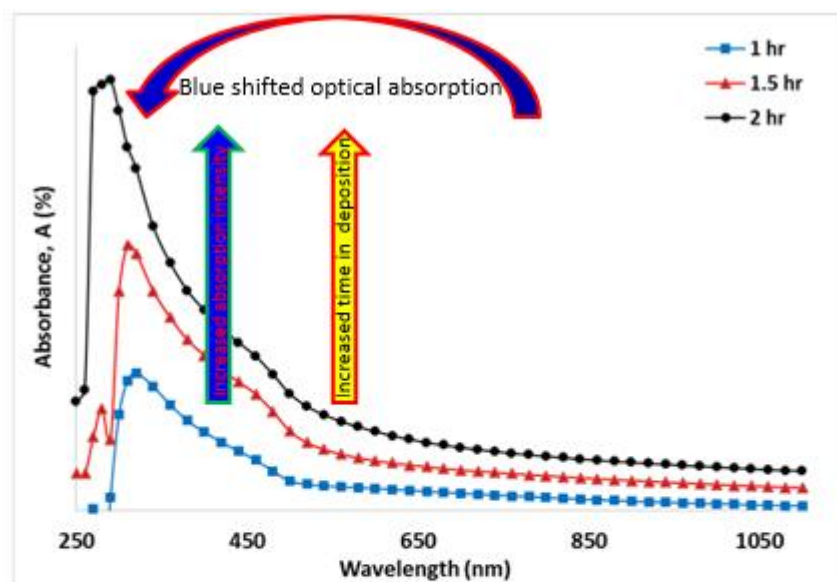
UV-Vis absorption spectra of Cd-Zn sulfide films deposited for 1 hr, 1.5 hr and 2 hr
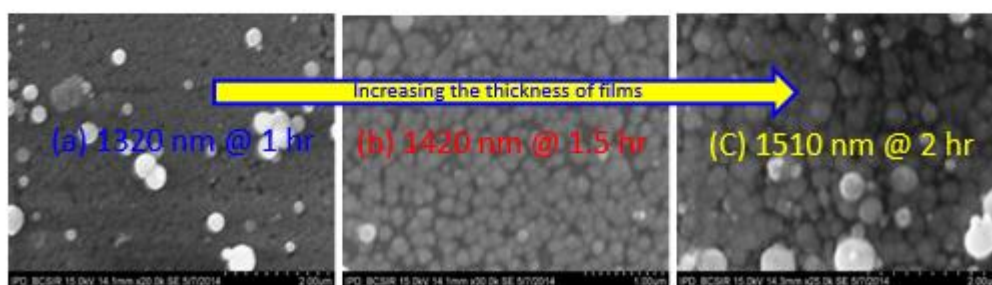
SEM images of Cd-Zn sulfide films deposited for (a) 1 hr, (b) 1.5 hr and (c) 2 hr

Highlights

- Cd-Zn sulphide films synthesized *via* chemical bath deposition technique were investigated for photovoltaic and optoelectronic applications.

- XRD studies show that Cd-Zn sulphide films are composed of nanocrystalline structure surrounded by the amorphous grain boundaries.

- Nanocrystalline structures of the films were confirmed by the SEM.

- The band gap of these films is a combination of composition and size

- E_U and σ studies ascribed the shrinkage of the solar absorption edges around the optical band-gaps.

ABSTRACT

In this article Cd-Zn sulphide thin films deposited onto soda lime glass substrates *via* chemical bath deposition (CBD) technique were investigated for photovoltaic applications. The synthesized films were investigated using X-ray diffraction (XRD), scanning electron microscopy (SEM), and ultraviolet visible (UV-Vis) spectroscopic methodologies. A higher degree of crystallinity of the films was attained with the increase of film thicknesses. SEM micrographs exhibited a partial crystalline structure with a particulate appearance surrounded by the amorphous grain boundaries. The optical absorbance and absorption coefficient of the films were also enhanced significantly with the increase in film thicknesses. Optical band-gap analysis indicated a monotonic decrease in direct and indirect band-gaps with the increase of thicknesses of the films. The presence of direct and indirect transitional energies due to the exponential falling edges of the absorption curves may either be due to the lack of long-range order or to the existence of defects in the films. The declination of the optical absorption edges was also confirmed *via* Urbach energy and steepness parameters studies.

Keywords: XRD; SEM; UV-Vis; crystallinity; band gap, absorption edges.

1. Introduction

Over the years, group II–VI semiconducting compounds have enjoyed a continuous interest by many research groups around the world due to a wide array of unique applications [1-4]. Generally these types of compounds are extensively used in solid-state physics especially in optoelectronics, photodetectors, low-voltage electroluminescent cathodes, heterojunction solar cells and photovoltaic cells with different polycrystalline absorber materials [5-11]. Within these classes, Cd-Zn sulphide based compounds have shown unique attraction due to their easy tuning of energy gap and lattice parameters [12, 13]. Furthermore, the energy gap of these films lies approximately 40 eV which is very optimal for photo-conducting materials, non-linear optics, and other optoelectronic devices. Remarkably, Cd-Zn sulphide films possess a band gap between CdS (2.42 eV) and ZnS (3.66 eV) which can be tuned by varying the ratio of Cd and Zn [14]. This spectacular energy band gap of these films guided them into window absorption losses and turned out a rise in short-circuit current in the solar cell. In addition to that, they are used in fabrication of *p-n* junctions without lattice mismatches but with the help of quaternary materials, like $CuInGaSe_2$ and $CuInS_2Se_2$ [15]. A large number of techniques such as chemical bath deposition (CBD) [16-19], dip-coating [20, 21], spray pyrolysis [22], proton exchange membrane [23], electro-active polymer [24], co-evaporation [25], thermal evaporation [26], solution growth technique [27], plasma polymerization [28, 29], reactive diffusion [30], sol-gel [31-34], chemical vapor deposition [35], unbalanced magnetron sputtering [36-39], and successive ionic layer adsorption and reaction [40] are extensively used for the deposition of film based products. Including the various deposition methods, extensive efforts are currently undergoing to comprehend fundamental properties of these films and their improvement using few of the above mentioned techniques. For example, effects of deposition parameters on the physical properties of $Cd_xZn_{1-x}S$ films deposited by spray pyrolysis method were investigated by Ilican *et al.* [41] and the film structures were found to be polycrystalline in nature. The same technique was also utilized by Selvan *et al.* for understanding the aging effect of Cd-Zn sulphide films [42]. Abbas *et al.* [43] reported the effect of thickness on structural and optical properties of $Zn_xCd_{1-x}S$ thin films prepared by chemical spray pyrolysis. Patidar *et al.* studied the structural, optical and electrical properties of such films developed by vacuum evaporation [44]. Dzhafarov *et al.* have investigated the structural, composition and optical absorption properties of Cd-Zn sulphide thin films deposited by Zn diffusions [30].

However, CBD method still retains wide usages due to combinaed advantages such as a non-vacuum, cost effective, reproducible, minimum material wastage, independent of sophisticated instrument and applied in large area of deposition at low temperature as well. The

4

basic principle of CBD is the deposition of thin films by controlled chemical reaction. Usually substrates are immersed in a solution containing the chalcogenide source, metal ion, and complexing agents. Ravangave *et al.* [45] studied the structural, morphological and electrical properties of $Cd_xZn_{1-x}S$ thin films deposited by CBD technique. XRD spectra demonstrated the hexagonal crystal structure of $Cd_xZn_{1-x}S$. The dark resistivity measurement showed that the films have high resistivity. The dark resistivity at room temperature was found to be of the order of ≥ 105 Ω cm for pure CdS and ≥ 106 Ω cm for $Cd_xZn_{1-x}S$ thin films. The dark resistivity was observed increased with Zn content as well. The similar method was also used to synthesize $Cd_{1-x}Zn_xS$ thin films by Isah [46] and found that the films had a transmittance between 75% and 85% and and an optical band gap within the range 2.8 - 3.4 eV. In view of the above, it is realized that Cd-Zn sulphide based films are of great interests to the scientific community. Even though large volumes of literature are available on Cd-Zn sulphide based films and related issues are comprehensively discussed both in experimental and theoretical view points however a clear understanding of the retrenchment of the optical absorption edges around the optical band-gaps is scant. Keeping these realities in mind, in the present work, we adopted CBD method to synthesize Cd-Zn sulphide films and carried out systematic studies on their structural, morphological, and various optical parameters to realize their variations with the film thicknesses. XRD, SEM and UV-Vis techniques were employed to investigate the Cd-Zn sulphide films and identifying the potential applications in photovoltaic and optoelectronic devices. In this regard, it is worth mentioning that a few other related work have been extensively reported in earlier studies [47, 48].

2. Materials and methods

2.1 Film synthesis process

All the glass wares were cleaned with both aqueous (HCl) and organic media (acetone, methanol) followed by an ultrasound bath and drying in oven. Cadmium acetate, zinc chloride, ammonium chloride and thiourea were dissolved together with the deionized water in a chemical bath (vessel) to make their corresponding 0.005 M, 0.02 M, 0.02 M and 0.04 M solution respectively. The pH of the solution was adjusted to 11 by the addition of 0.2 M ammonium hydroxide with constant stirring. The temperature of the chemical bath was kept at 80 °C with the aid of a hot plate stirrer. A thermometer was used for continuous monitoring of the temperature of the chemical bath. For thin film synthesis, the soda lime glass substrates were vertically placed into the chemical bath containing a solution of 120 ml and allowed them for deposition for the periods of 1.0 h, 1.5 h and 2.0 h respectively. After elapsing the desired deposition time, the glass

substrates were removed from the chemical bath solution and immediately rinsed with deionized water in such a way that no loosely-bound powder was left onto the films surface. Finally, the films were dried in an open atmosphere for a period of couple of hours. The thicknesses of the deposited films were measured by the weigh difference method.

The chemical processes involved in the formation of ZnS and CdS are shown in the following chemical reactions:

$$NH_3 + H_2O = NH_4^+ + OH^-$$

$$Zn^{2+} + 4NH_3 = [Zn(NH_3)_4]^{2+}$$

$$CS(NH_2)_2 + 2OH^- = S^{2-} + CN_2H_2 + 2H_2O$$

$$[Zn(NH_3)_4]^{2+} + S^{2-} = ZnS\ (s) + 4NH_3$$

$$Cd^{2+} + 4NH_3 = [Cd(NH_3)_4]^{2+}$$

$$[Cd(NH_3)_4]^{2+} + S^{2-} = CdS\ (s) + 4NH_3$$
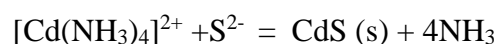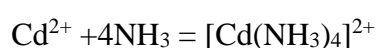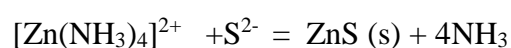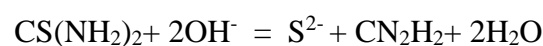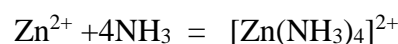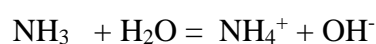
2.2 Measuring the films thicknesses

Thickness of the films can be measured either by *in-situ* monitoring of the rate of deposition, or other techniques after fabrication. There are several methods to estimate the thickness of the deposited films with varying degree of accuracy. One can choose a method on the basis of their convenience, simplicity and reliability. Since the film thicknesses are generally in the order of wavelength of light, various types of optical interference phenomena are involved in thickness measurements. Nowadays commonly used *in-situ* film thickness measurement systems are, multiple-beam interferometry, Michelson interferometer, and using a hysteresis graph. In this study, we have adopted a Multiple-beam interferometry method to measure the thickness of the films. A UV-1200 spectrophotometer (Shimadzu Corporation, Japan) was used to measure the film thickness using a programmable data pack. Table 1 displays the thickness values of CdZnS films deposited for 1.0 hr, 1.5 hr, and 2.0 hr.

2.3 XRD measurements

XRD is a non-destructive analytical tool primarily used for phase identification of a crystalline material to provide information with the crystallinity, orientation, lattice constants and phase of crystals. X-ray diffraction (XRD) data of the films were collected out using PANalytical X'Pert Pro diffractometer that uses a Cu-K_α X-ray source of wavelength, $\lambda = 0.15418$ nm. PANalytical X'Pert Pro diffractometer consists of three equally important parts namely X-Ray tube (X-Ray source), rotating sample platform (goniometry) and detector. The other three parts of this machine are the collimator, filter and monochromator. X-rays were emitted from an X-ray

6

tube which sits at one end of one arm of goniometer stage. Generally, X-rays are incident onto the films at an angle θ with respect to the film surface, and collected by a detector situated in the goniometer arm at 2θ distance along the direction of the incident [49]. The XRD machine was operated at a power of 40 kV and 40 mA, with high temperature attachment up to 1600 °C. The XRD data were recorded in the angular range of $10° \leq 2\theta \leq 60°$ in steps of $0.02°$.

2.4 SEM imaging of the films

The surface morphology of the as deposited Cd-Zn sulphide films was performed *via* a high resolution (3 nm) and low vacuum analytical scanning electron microscope (JEOL JSM-6490LA) installed at IPD, BCSIR in Dhaka. The low vacuum mode of the system allows to observe the specimens which cannot be viewed at high vacuum due to excessive water content or due to nonconductive surface. The take-off angle for the JSM-6490ALA was 35°, with an analytical working distance of 10 mm. Prior to SEM imaging, the film surfaces were coated with a thin layer of gold by sputtering (AGAR Auto Sputter Coater).

2.5 Optical measurements technique

The optical properties of Cd-Zn sulphide thin films were conducted by a dual beam UV-Vis spectrophotometer (SHIMADZU UV-1601, JAPAN), installed at PP and PDC, BCSIR in Dhaka, in the wavelength range of 190-1100 nm at room temperature. Prior recording the absorption data of the films, a blank glass substrate was used as the reference. After base line correction, the films were placed vertically onto the sample holder and illuminated by a monochromatic beam of light to record the absorption spectra. Acquired absorption spectra were used to calculate the energy band-gap values and other optical studies such as Urbach energy, and steepness parameters.

3. Results and discussion

3.1 XRD studies of the Cd-Zn sulphide films

XRD spectra of the Cd-Zn sulphide films with different thicknesses are displayed in Fig. 1. The XRD spectra did not reveal well-defined peaks, indicating a disordered state of the materials having a mixture of nanocrystalline and amorphous phases. Inspection of XRD spectra, from all three films, show that the intensity of the diffraction peaks significantly increased with the increase in film thicknesses. This feature confirms the nanocrystalline phases of the films are attained with the increased thicknesses. Film deposited for 1 hour shows the principal peak at $2\theta = 26.53°$ due to a (002) reflection, and another peak at $2\theta = 28.50°$ corresponding to a (101) reflection. Few other reflection peaks (such as (100), (110), (103) and (112)) at lower and higher

angle sides were also identified. All these features are consistent with the JCPDS 00-049-1302, with a hexagonal lattice system of space group *P63mc* (186). Similar features were also realized with the films deposited for 1.5 and 2 hrs. However, for 2 hr deposited films, the peaks detected for (002), (110) and (112) reflection planes possess significantly higher intensity then those deposited for 1 and 1.5 hr. This clearly states that the higher degree of crystallinity has been achieved with films deposited for the period of 2 hr. The (002) peak gives the lattice matching to the chalcogenide semiconductor, such as $CuInGaSe_2$ and $CuIn(Se_xS_{1-x})_2$, that have wide-spread applications in solar cell devices for a superior cell performance [50].

The average crystallite size, *D* of the films were calculated *via* Scherrer's formula,

$$D = \frac{C\lambda}{\beta Cos\theta} \tag{1}$$

where *C* is a constant equal to 0.94, λ is the X-ray wavelength of CuK_α radiation (= 0.15418 nm), β (in radian) is the full width at half maximum (FWHM), and θ is the Bragg's diffraction angle. The lattice constants *a* and *c* of Cd-Zn sulphide films were calculated using XRD data *via* following Eq. (2).

$$\frac{1}{d^2} = \frac{4}{3}\left(\frac{h^2+hk+k^2}{a^2}\right) + \frac{l^2}{c^2} \tag{2}$$

The lattice constants and average crystallite size of these films at different film thicknesses are enumerated in Table 1. Accoring to the crystallite size and lattice constant values presented in Table 1, it clearly indicates that the synthesized Cd-Zn sulphide films are in nanocrystalline phases.

3.2   Surface morphology of Cd-Zn sulphide *films*

Scanning electron microscopy (SEM) studies were carried out to inspect the surface morphology, grain size and uniformity of Cd-Zn sulphide films. Fig. 2 includes the SEM images of Cd-Zn sulphide films deposited onto glass substrates for 1, 1.5 and 2 hrs in air. The grain morphology of the films were examined at different magnifications. It has been observed that the grain size increases with increasing deposition times. For 1 hr period deposited films, the average grain sizes are about 150 nm while the films deposited for 2 hr have an average grain size of 205 nm. This reveals that more materials are dumped onto the glass substrates to yield a thicker thin films together with larger grain size and surface area. The grains seem to be isolated from each other with a well-defined gaps in between. It is assumed that the white grains are originated from cadmium material whereas the black grains arisen due to from Zn-content. Further investigations demonstrated that the number of grains of Cd-content is remarkably less than that of Zn material.

8

This is because of the replacement of Zn atoms by the Cd atoms. Nanostructure formations of $CdSe_{0.6}Te_{0.4}$ films, deposited *via* electrochemical route at different deposition times, were confirmed using FESEM studies [46]. As a result of these nanostructures these films were found to facilitate the light absorption behaviour and thus can participate in multiple scattering and absorption processes which in turn demonstrate promising improvement in the power conversion efficiency of solar havesting devices [47]. In another report, the surface morphological study of electrochemically synthesized $Cd_{0.3}Zn_{0.7}S$ films was conceded by FESEM imaging. Nanospheres like nanocrystalline morphologies of the films were observed all over the substrate's surface. Authors argued that these nanospheres like surface morphologies of these films are responsible for altercation of electron–hole couple in electrolytic bath that is also viable for solar energy harnessing [48]. Since, in solar cell applications, the surface of p-type layer is kept exceedingly thin that solar radiation can easily penetrate the surface of the films. This thin layer is connected to the positive terminal of the solar device. Observed granular like surface morphology is responsible for the densely packed surface morphology and a larger number of grains can be accommodated in smaller surface area of the films that is potentially ideal for a solar cell application view point [45].

3.3   Optical studies of as deposited Cd-Zn sulphide films

3.3.1   Solar absorbance and absorption coefficient of Cd-Zn sulphide *films*

The optical absorption edges of the films were analyzed *via* UV-Vis spectroscopy. Fig. 3 illustrates the UV-Vis absorbance spectra, acquired in the wavelength range of 250-1100 nm, of the films for various thicknesses at room temperature. The optical absorbance values of these films are displayed in Table 2.

From Fig. 3 and Table 2, it is seen that the optical absorbance of the films increases significantly with the increase in thicknesses of the films. Broadening features of the absorption peaks are also observed with the increase of thickness. The absorption intensities rise sharply in the wavelength region of 250-420 nm, attains its maximum value of 95.4% and then drops rapidly up to 850 nm. Strong absorption around 260-320 nm is ascribed to electronic inter-band transitions from the filled sulphide (S3p) valence band through to the empty conduction band [51]. Well-defined absorption edges indicate a good quality of the films, and the ternary films are comprised by a solid solution [52]. This is because of the higher degree of crystallizations of the films is attained with the higher deposition times. The UV-Vis spectra also demonstrate that, with the increase in film thicknesses, the absorption edges of the films shift to high frequency end (or so called "blue shifted"). At the same time, a clear increase in the magnitudes in the absorption

edges is noticed with the increase in deposition times of the films. The increase in absorption intensities at higher deposition times reveals the thicker depositions of the Cd-Zn sulphide films. It is also assumed that higher degree of optical absorption and blue shifting of the absorption edges with increased film thickness are associated with quantum size effect [53]. The higher values of solar absorption at higher film thickness are due to the presence of defects and vacancies as reflected from SEM images (see Fig. 2). Optical studies attribute that all the films are highly absorptive with both direct and indirect types of transitions. These features are extensively discussed in the optical band gap (E_g) analysis section (see section 3.3.2).

The absorption coefficient, α of the films was estimated, from absorbance data corresponding to different photon energies at room temperature, using the following relation [54],

$$\alpha = 2.3026 \; \frac{A}{d} \tag{3}$$

where, $A = log_{10}\left(\frac{I_0}{I}\right)$ is the absorbance at a specific wavelength, and d is the thickness of the films. The spectral dependence of α on the photon energy, $h\nu$ are presented in the following Fig. 4. The spectral dependence of the absorption coefficient on the photon energy helps to understand the band structure and electronic transitions involved in the absorption processes. Absorption edges evolved at 1.3eV and sharply rises from 2.5eV. The absorption spectra have two slopes in the observed photon energy range that indicate the presence of direct and indirect optical transitions in the Cd-Zn sulphide films. These falling edges are assumed to be either due to lack of long-range order, or due to the presence of localized defects around the film surfaces.

3.3.2   Optical band-gaps in Cd-Zn sulphide films

In crystalline and amorphous materials, the involved optical transition can be determined on the basis of the dependence of α on photon energy, $h\nu$, *via* Tauc relation [28],

$$\alpha h\nu = C\left(h\nu - E_{opt}\right)^{n} \tag{4}$$

where, $h\nu$ is the incident photon energy, h Planck's constant, ν the frequency of the incident solar radiation, C an energy independent constant and is a measure of the steepness of band tail density of states (Urbach region), E_{opt} the energy of optical band-gap, and n is an index depending on the type of optical transition involved in the photon absorption process. The index n equals 0.5, 2, 1.5 and 3 for allowed direct, allowed indirect, forbidden direct and forbidden indirect transitions, respectively [55]. Thus, the indirect band-gap energy, E_i can be estimated by plotting $(\alpha h\nu)^{1/2}$ versus $h\nu$ curves and extrapolating the linear portion of the curve to $(\alpha h\nu)^{1/2} = 0$. The direct band-gap energy, E_d is computed by plotting $(\alpha h\nu)^2$ with respect to the photon energy and extrapolating the linear portion of the curve to $(\alpha h\nu)^2 = 0$ along the photon energy axis.

10

In Fig. 5, $(\alpha h\nu)^2$ is plotted as a function of $h\nu$ to estimate E_d of Cd-Zn sulphide films. The direct band-gap energy of Cd-Zn sulphide films was calculated using the intercept of the linear part of the curves extrapolated to zero along the *X*-axis [56]. The direct energy band-gap values of as deposited Cd-Zn sulphide thin films with various thicknesses are documented in Table 3. In a similar fashion mentioned above, using Fig. 6 (plots of $(\alpha h\nu)^{1/2}$ vs $h\nu$) , the indirect energy band-gap values of as deposited Cd-Zn sulphide films with various thicknesses are computed and presented in Table 3. It is found that the energy band gap is thickness dependent. This may be due to the possibility of structural defects in the films that took place during the time of their preparation, which could give rise to the defect states near the conduction band in the band gap. The linear landscape of the Tauc plots (see Fig. 5 and Fig. 6) at the absorption edges established that the Cd-Zn sulphide films possess semiconductor nature. The direct band gaps of the as-deposited films varied from 3.10 to 2.45 eV; whereas, indirect band gaps varied from 1.60 to 1.20 eV. The decreased band gap is due to the increased crystalline nature of the films [57]. It is also proposed that the increase of energy band-gaps of these films is due to the increase in grain size. The reduction of the direct energy band-gap is related to the band tailing triggered by the disorder of the films. The optical band-gaps of the films are, generally, affected by two factors: the inherent band gap of the material and a tail due to disorder [58]. In semiconducting materials optical band-gaps are significantly influenced by the defects, residual strain, impurities, and disorders of grain boundaries [59]. It is also known that the tensile strains result in a decrease in energy band-gaps due to the extended lattice, while compressional strains result to enhance the optical band-gaps because of the lattice compressions. By using longer deposition times the carrier concentration increases and the optical band-gap decreases. As a result, shrinking in the optical band-gaps of CdZn-sulphide films come into play. It is also believed that the higher deposition times results to increase the particle size and thereby reducing the optical band-gaps owing to the decreasing contribution of particle size confinement effect [60].

3.3.3   *Urbach energy and steepness parameters in Cd-Zn* sulphide *films*

Generally, the spectral dependence of the absorption coefficients are studied at photon energies less than the energy band-gap of the films *i.e*., in a region so called Urbach spectral tail that characterizes the slope of the exponential edge and is expressed as [61],

$$\alpha = \alpha_0 \exp\left(\frac{E}{E_U}\right) \qquad (5)$$

where α_0 is a temperature dependent constant and E_U, the Urbach energy.

The E_U can be evaluated as the width of the exponential absorption edge or as the width of the tails of localized states. Urbach plots of log(α) vs hv for Cd-Zn sulphide films of different thicknesses are shown in Fig. 7. An emperical relationship, $E_U = [d(\ln\alpha)/d(hv)]^{-1}$ was used to estimate the Urbach energies. The corresponding Urbach energy values as estimated *via* this relationship are listed in Table 4. The plots of log(α) vs hv give out linear curves whose slope provide with the Urbach energy (E_U), typically known as the width of the tails of localized states in the energy band-gaps of the films. It is clearly seen that the values of E_U, which essentially indicates the band width of the localized states, increases as the thicknesses of the films are increased. An increase in the energy band-gaps of an amorphous structure is, generally, associated with the decrease of the band tails around the energy band-gaps. This phenomena is associated with the increase in the degree of crystallinity and a decrement in density of defect states [62].

The steepness parameter, σ characterizing the broadening of the optical absorption edges due to electron-phonon or exciton-phonon interactions, was calculated by the following equation [63],

$$\sigma = \frac{k_B T}{E_U} \qquad (6)$$

where k_B is the Boltzmann constant and T is the absolute temperature in kelvin. The calculated room temperature steepness parameters, σ , are listed in Table 4. From Table 4, it is seen that the absorption edges of the Cd-Zn films are narrowed down with the gradual increase in film thicknesses. The 'steepness parameter' σ indicates the broadening or shrinkage of the optical absorption edges arise from the electron-phonon/exciton–phonon interactions. The increase in the Eu values is associated with the increase of localized states originated from the non-radiative recombination centres [64]. These localized states might be resulted either from the vacancies or dislocation defects of the films. It is established that optical absorption response of these films are strongly dependent on the presence of localized states in the forbidden band gap of materials. The shapes of absorption edges provides with substantial evidence on the localized states and disorder effects. In amorphous structures, these localized states play even more important roles. Since Urbach energy indicates the measure of the width of localized states associated with nanocrystalline or amorphous films around the optical band-gap, the exponential dependence E_U on hv is assumed to be initiated from the random variations of internal fields related to the structural disorders [65]. With longer deposition times, the carrier concentration increases and the energy band-gap decreases. This phenomenon is well supported by Moss–Burstein effect [66]. The red shift of the absorption edges is related to the *p–d* spin-exchange interactions between the band electrons and the localized *d* electrons of Cd^{2+} ions as reported by

Diouri *et al*. [67]. Consequently, the optical absorption edges of the Cd-Zn sulphide films are shrinking around the optical band-gaps.

4. Conclusions

Cd-Zn sulphide films, synthesized onto soda lime glass substrates *via* chemical bath deposition technique, were investigated for their structural morphology and optical analysis. X-ray diffraction studies showed that Cd-Zn sulphide films are composed of nanocrystalline structure embedded by the amorphous grain boundaries. Nanocrystalline structures of the films were confirmed by the SEM studies where the grain sizes were in the nanoscale range. The solar absorption of a material resembles the electron excitation from valance band to conduction band is successfully used to regulate the nature and value of the optical band gap. The band gap of these films is a combination of alloying effect (composition) and quantum confinement effect (size) and fluctuates largely at low crystallite size. The solar absorbance, absorption coefficient were increased with the increase in deposition time while optical band gaps of the films were significantly altered. Urbach energy values and steepness parameter studies ascribed that with the monotonic increase in films thicknesses, the shrinkage of the solar absorption edges of the films become predominant around the optical band-gaps. This information would play a crucial role in the utilization of these materials to design a suitable window material for solar cell devices and optoelectronic applications.

References

[1] S. Chattopadhyay, P. Sen, J. Thomas Andrews, P. Kumar Sen, Semiconductor core-shell quantum dot: A low temperature nano-sensor material, Journal of Applied Physics, 111 (2012) 034310.

[2] M. Husain, B. Pal Singh, S. Kumar, T.P. Sharma, P.J. Sebastian, Optical, electrical and structural investigations on $Cd_{1-x}Zn_xSe$ sintered films for photovoltaic applications, Solar Energy Materials and Solar Cells, 76 (2003) 399-415.

[3] J.A. Kausalya, V. Joseph, S. Krishnakumar, Synthesis of cadmium selenide nanoparticles by wet chemical method, Applied Chemistry, 55A (2013) 13036-13038.

[4] K. Raksha, S. Ananda, An investigation on: kinetics of photo catalysis, electrical property and biological activity of electrochemically synthesized ZnS and Ru: ZnS nano photocatalysts, Journal of Applicable Chemistry (Lumami, India), 3 (2014) 397-412.

[5] J. Aguilar-Hernández, J. Sastre-Hernández, N. Ximello-Quiebras, R. Mendoza-Pérez, O. Vigil-Galán, G. Contreras-Puente, M. Cárdenas-García, Photoluminescence studies on CdS-CBD films grown by using different S/Cd ratios, Thin Solid Films, 511–512 (2006) 143-146.

[6] S.A. Al Kuhaimi, Z. Tulbah, Structural, Compositional, Optical, and Electrical Properties of Solution-Grown $Zn_xCd_{1-x}S$ Films, Journal of The Electrochemical Society, 147 (2000) 214-218.

[7] P. Asogwa, variation of optical properties with post deposition annealing in chemically deposited CdZnS thin films, Chalcogenide Letters, 7 (2010) 501-508.

[8] T.P. Kumar, K. Sankaranarayanan, Growth and characterization of CdZnS thin films by short duration micro wave assisted chemical bath deposition, Chalcogenide Letters, 6 (2009) 555-562.

[9] Y. Raviprakash, K.V. Bangera, G.K. Shivakumar, Preparation and characterization of $Cd_xZn_{1-x}S$ thin films by spray pyrolysis technique for photovoltaic applications, Solar Energy, 83 (2009) 1645-1651.

[10] J.A. Rojas, A.I. Oliva, A Double Energy Transition of Nanocrystalline $Cd_xZn_{1-x}S$ Films Deposited by Chemical Bath, Materials and Manufacturing Processes, 30 (2015) 785-792.

[11] J. Torres, G. Gordillo, Photoconductors based on $Zn_xCd_{1-x}S$ thin films, Thin Solid Films, 207 (1992) 231-235.

[12] M. Ashokkumar, S. Muthukumaran, Size Dependent Structural and Optical Properties of $Cd_{0.9}Zn_{0.1}S$ Thin Films, Physics Procedia, 49 (2013) 137-144.

[13] T.P. Kumar, S. Saravanakumar, K. Sankaranarayanan, Effect of annealing on the surface and band gap alignment of CdZnS thin films, Applied Surface Science, 257 (2011) 1923-1927.

[14] S.R. Deo, A.K. Singh, L. Deshmukh, M. Abu Bin Hasan Susan, Metal Chalcogenide Nanocrystalline Solid Thin Films, Journal of Electronic Materials, 44 (2015) 4098-4127.

[15] S. Ezugwu, F. Ezema, P. Asogwa, Synthesis and Characterization of Ternary CuSbS2 Thin Films: Effect of Deposition Time", Chalcogenide Letters, 7 (2010) 341-348.

[16] S.D. Chavhan, S. Senthilarasu, S.-H. Lee, Annealing effect on the structural and optical properties of a $Cd_{1-x}Zn_xS$ thin film for photovoltaic applications, Applied Surface Science, 254 (2008) 4539-4545.

[17] S. Tec-Yam, R. Patiño, A.I. Oliva, Chemical bath deposition of CdS films on different substrate orientations, Current Applied Physics, 11 (2011) 914-920.

[18] S. Tec-Yam, J. Rojas, V. Rejón, A.I. Oliva, High quality antireflective ZnS thin films prepared by chemical bath deposition, Materials Chemistry and Physics, 136 (2012) 386-393.

[19] M.S. Mina, H. Kabir, M.M. Rahman, M.A. Kabir, M. Rahaman, M.S. Bashar, M.S. Islam, A. Sharmin, F. Ahmed, Optical and Morphological Characterization of BaSeThin Films Synthesized via Chemical Bath Deposition, IOSR Journal of Applied Physics, 4 (2013) 30-35.

[20] A. Amri, Z.-T. Jiang, N. Wyatt, C.-Y. Yin, N. Mondinos, T. Pryor, M.M. Rahman, Optical properties and thermal durability of copper cobalt oxide thin film coatings with integrated silica antireflection layer, Ceramics International, 40 (2014) 16569-16575.

14

[21] A. Millar, M.M. Rahman, Z.-T. Jiang, Review of Sol-Gel Derived Mixed Metal Oxide Thin Film Coatings with the Addition of Carbon Materials for Selective Surface Applications, Journal of Advanced Physics, 3 (2014) 179-193.

[22] L. Ravangave, U. Biradar, S. Misal, The Effect of Ionic Composition on Structural and Optical Properties of CdxZn1-xS Thin films Grown by Spray pyrolysis, International J. of Scientific and Research Publications, 2 (2012) 2250-3153.

[23] Khadiza Begam, Md. Alamgir Kabir, M. Mahbubur Rahman, Md. Abul Hossain, M.A. Khan, Properties of Proton Exchange Membranes Poly-ethylene Terephthalate (PET) Films Developed by Gamma Radiation Induced Grafting and Sulfonation Technique, Physics and Materials Chemistry, 1 (2013) 13-20.

[24] Md. Alamgir Kabir, Khadiza Begam, M. Mahbubur Rahman, Fahmida Parvin, Md. Arifur Rahman, Jahid M M Islam, Md. Abul Hossain, Farid Ahmed, M.A. Khan., Characterization of Electroactive Polymer Composite Films based on Gelatin and Poly 2-(3-thienyl)-ethoxy-4-butylsulfonate (PTEBS), ARPN Journal of Science and Technology, 3 (2013) 639-646.

[25] J.-H. Lee, W.-C. Song, J.-S. Yi, K.-J. Yang, W.-D. Han, J. Hwang, Growth and properties of the $Cd_{1-x}Zn_xS$ thin films for solar cell applications, Thin Solid Films, 431–432 (2003) 349-353.

[26] M.A. Mahdi, Z. Hassan, J.J. Hassan, S.S. Ng, S.J. Kasim, Preparation and characterization of $Zn_xCd_{1-x}S$ ternary alloys micro/nanostructures grown by thermal evaporation, Materials Research Express, 2 (2015) 016501.

[27] D.M. Jeroh, A Study on The Structural, Optical and Electrical Properties of CuSbS2 Thin Films and Possible Applications, International Journal of Thin Films Science and Technology, 2 (2013) 43-52

[28] H. Kabir, M.M. Rahman, T.S. Roy, A. Bhuiyan, Structural and optical properties of plasma polymerized pyromucic aldehyde thin films, International Journal of Mechanical & Mechatronics Engineering, 12 (2012) 30-34.

[29] H. Kabir, A.H. Bhuiyan, M.M. Rahman, Understanding the charge carrier conduction mechanisms of plasma-polymerized 2-furaldehyde thin films via DC electrical studies, Thin Solid Films, 609 (2016) 35-41.

[30] T.D. Dzhafarov, F. Ongul, I. Karabay, Formation of CdZnS thin films by Zn diffusion, Journal of Physics D: Applied Physics, 39 (2006) 3221.

[31] A. Amri, X. Duan, C.Y. Yin, Z.T. Jiang, M.M. Rahman, T. Pryor, Solar absorptance of copper-cobalt oxide thin film coatings with nano-size, grain-like morphology: Optimization and synchrotron radiation XPS studies, Applied Surface Science, 275 (2013) 127-135.

[32] A. Amri, Z.T. Jiang, P.A. Bahri, C.Y. Yin, X. Zhao, Z. Xie, X. Duan, H. Widjaja, M.M. Rahman, T. Pryor, Surface electronic structure and mechanical characteristics of copper-cobalt oxide thin film coatings: Soft X-ray synchrotron radiation spectroscopic analyses and modeling, Journal of Physical Chemistry C, 117 (2013) 16457-16467.

[33] A. Amri, Z.T. Jiang, X. Zhao, Z. Xie, C.Y. Yin, N. Ali, N. Mondinos, M.M. Rahman, D. Habibi, Tailoring the physicochemical and mechanical properties of optical copper-cobalt oxide thin films through annealing treatment, Surface and Coatings Technology, 239 (2014) 212-221.

[34] A. Amri, Z.-T. Jiang, C.-Y. Yin, A. Fadli, M.M. Rahman, S. Bahri, H. Widjaja, N. Mondinos, T. Herawan, M.M. Munir, G. Priyotomo, Structural, optical, and mechanical properties of cobalt copper oxide coatings synthesized from low concentrations of sol–gel process, physica status solidi (a), (2016) DOI: 10.1002/pssa.201600207.

[35] P.B. Smith, Low temperature, low pressure CdZnS films produced by metalorganic chemical vapor deposition, Journal of Vacuum Science & Technology A, 10 (1992) 897-902.

[36] M.M. Rahman, Z.-T. Jiang, X. Duan, Z. Xie, A. Tadich, Z.-f. Zhou, N. Mondinos, C.-Y. Yin, M. Altarawneh, B.Z. Dlugogorski, NEXAFS N K-edge study of the bonding structure on Al/Si doped sputtered CrN coatings, Journal of Alloys and Compounds, 661 (2016) 268-273.

[37] M.M. Rahman, Z.-T. Jiang, Z. Xie, X. Duan, Z.-f. Zhou, P.C. Wo, C.-Y. Yin, N. Mondinos, Q. Gu, H. Widjaja, K. Jack, A. Yago, A. Amri, Understanding Local Bonding Structures of Ni-

15

Doped Chromium Nitride Coatings through Synchrotron Radiation NEXAFS Spectroscopy, The Journal of Physical Chemistry C, 118 (2014) 18573-18579.

[38] M.M. Rahman, Z.-T. Jiang, Z.-f. Zhou, Z. Xie, C.Y. Yin, H. Kabir, M.M. Haque, A. Amri, N. Mondinos, M. Altarawneh, Effects of annealing temperatures on the morphological, mechanical, surface chemical bonding, and solar selectivity properties of sputtered TiAlSiN thin films, Journal of Alloys and Compounds, 671 (2016) 254-266.

[39] M. Mahbubur Rahman, A. Duan, Z.-T. Jiang, Z. Xie, A. Wu, A. Amri, B. Cowie, C.-Y. Yin, Near-edge X-ray absorption fine structure studies of $Cr_{1-x}M_xN$ coatings, Journal of Alloys and Compounds, 578 (2013) 362-368.

[40] H. Pathan, C. Lokhande, Deposition of metal chalcogenide thin films by successive ionic layer adsorption and reaction (SILAR) method, Bulletin of Materials Science, 27 (2004) 85-111.

[41] S. Ilican, M. Caglar, Y. Caglar, The effect of deposition parameters on the physical properties of $Cd_xZn_{1-x}S$ films deposited by spray pyrolysis method, Journal of Optoelectronics and Advanced Materials, 9 (2007) 1414-1417.

[42] G. Selvan, M.P. Abubacker, K. Usharani, A.R. Balu, Precursor aging effect on the properties of CdZnS films, Surface Engineering, 32 (2016) 212-217.

[43] N.K. Abbas, L.K. Abbas, Effect Of Thickness On Structural And Optical Properties Of $Zn_xCd_{1-x}S$ Thin Films Prepared By Chemical Spray Pyrolysis, International Journal of Thin Films Science and Technology, 2 (2013) 127-132.

[44] D. Patidar, N.S. Saxena, T.P. Sharma, Structural, optical and electrical properties of CdZnS thin films, Journal of Modern Optics, 55 (2008) 79-88.

[45] L. Ravangave, U. Biradar, Study of structural, Morphological and Electrical Properties of $Cd_xZn_{1-x}S$ Thin Films, IOSR J. of Applied Physics, 3 (2013) 41-47.

[46] K.U. Isah, Optical and Morphological Studies of Chemical Bath Deposited Nanocrystalline $Cd_{1-x}Zn_xS$ Thin Films, Materials Sciences and Applications, 4 (2013) 287-292.

[47] S.K. Shinde, G.S. Ghodake, D.P. Dubal, G.M. Lohar, D.S. Lee, V.J. Fulari, Structural, optical, and photo-electrochemical properties of marygold-like CdSe0.6Te0.4 synthesized by electrochemical route, Ceramics International, 40 (2014) 11519-11524.

[48] H.D. Dhaygude, S.K. Shinde, D.P. Dubal, M.C. Rath, V.J. Fulari, Effect of electron beam irradiation on electro synthesized hexagonal Cd0.3Zn0.7S nanosphere with excellent application in solar cell, Applied Surface Science, 368 (2016) 1-7.

[49] H.P. Klug, L.E. Alexander, X-Ray Diffraction Procedures, Wiley, New York, USA, 1974.

[50] S.V. Borse, S.D. Chavhan, R. Sharma, Growth, structural and optical properties of $Cd_{1-x}Zn_xS$ alloy thin films grown by solution growth technique (SGT), Journal of Alloys and Compounds, 436 (2007) 407-414.

[51] K. Ramasamy, M.A. Malik, M. Helliwell, J. Raftery, P. O'Brien, Thio- and Dithio-Biuret Precursors for Zinc Sulfide, Cadmium Sulfide, and Zinc Cadmium Sulfide Thin Films, Chemistry of Materials, 23 (2011) 1471-1481.

[52] E.A. Sanchez-Ramirez, M.A. Hernandez-Perez, J. Aguilar-Hernandez, E. Rangel-Salinas, Nanocrystalline $CdS_{1-x}Se_x$ alloys as thin films prepared by chemical bath deposition: Effect of x on the structural and optical properties, Journal of Alloys and Compounds, 615, Supplement 1 (2014) S511-S514.

[53] M. Ashok Kumar, S. Muthukumaran, Effect of deposition time on structural, optical and photoluminescence properties of $Cd_{0.9}Zn_{0.1}S$ thin films by chemical bath deposition method, Journal of Materials Science: Materials in Electronics, 24 (2013) 2858-2865.

[54] N. Gaewdang, T. Gaewdang, Investigations on chemically deposited $Cd_{1-x}Zn_xS$ thin films with low Zn content, Materials Letters, 59 (2005) 3577-3584.

[55] S. Islam, M. Hossain, H. Kabir, M. Rahaman, M. Bashar, M. Gafur, A. Kabir, M. Bhuiyan, F. Ahmed, N. Khatun, Optical, Structural and Morphological Properties of Spin Coated Copper Zinc Tin Sulfide Thin Films, International Journal of Thin Films Science and Technology, 4 (2015) 155-161.

16

[56] L. Ravangave, U. Biradar, Study of Optical Parameters of Chemical Bath Deposited $Cd_{1-x}Zn_xS$ Thin Films, Materials Physics and Mechanics, 16 (2013) 25-33.

[57] S. Chavhan, R.P. Sharma, Growth, structural and optical transport properties of nanocrystal $Zn_{1-x}CdS$ thin films deposited by solution growth technique (SGT) for photosensor applications, Journal of Physics and Chemistry of Solids, 66 (2005) 1721-1726.

[58] M. Ichimura, F. Goto, E. Arai, Structural and optical characterization of CdS films grown by photochemical deposition, Journal of Applied Physics, 85 (1999) 7411-7417.

[59] Y.G. Wang, S.P. Lau, H.W. Lee, S.F. Yu, B.K. Tay, X.H. Zhang, H.H. Hng, Photoluminescence study of ZnO films prepared by thermal oxidation of Zn metallic films in air, Journal of Applied Physics, 94 (2003) 354-358.

[60] A.J. Peter, C.W. Lee, Electronic and optical properties of CdS/CdZnS nanocrystals, Chinese Physics B, 21 (2012) 087302.

[61] G. Hodes, Chemical Solution Deposition of Semiconductor Films, Marcel Dekker, Inc., New York, USA, 2003.

[62] J.L. Vossen, W. Kern, Thin Film Processes II, Academic Press, Inc., Boston, USA, 1991.

[63] M.A. Contreras, M.J. Romero, R. Noufi, Characterization of $Cu(In,Ga)Se_2$ materials used in record performance solar cells, Thin Solid Films, 511–512 (2006) 51-54.

[64] W.F. Lim, H.J. Quah, Z. Hassan, R. Radzali, N. Zainal, F.K. Yam, Alteration of structural and optical properties in quaternary $Al_{0.1}In_{0.1}Ga_{0.8}N$ films using ultraviolet assisted photo-electrochemical etching route, Journal of Alloys and Compounds, 649 (2015) 337-347.

[65] F. Yakuphanoglu, M. Arslan, The fundamental absorption edge and optical constants of some charge transfer compounds, Optical Materials, 27 (2004) 29-37.

[66] B. Joseph, P.K. Manoj, V.K. Vaidyan, Studies on the structural, electrical and optical properties of Al-doped ZnO thin films prepared by chemical spray deposition, Ceramics International, 32 (2006) 487-493.

[67] J. Diouri, J.P. Lascaray, M.E. Amrani, Effect of the magnetic order on the optical-absorption edge in $Cd_{1-x}Mn_xTe$, Physical Review B, 31 (1985) 7995-7999.
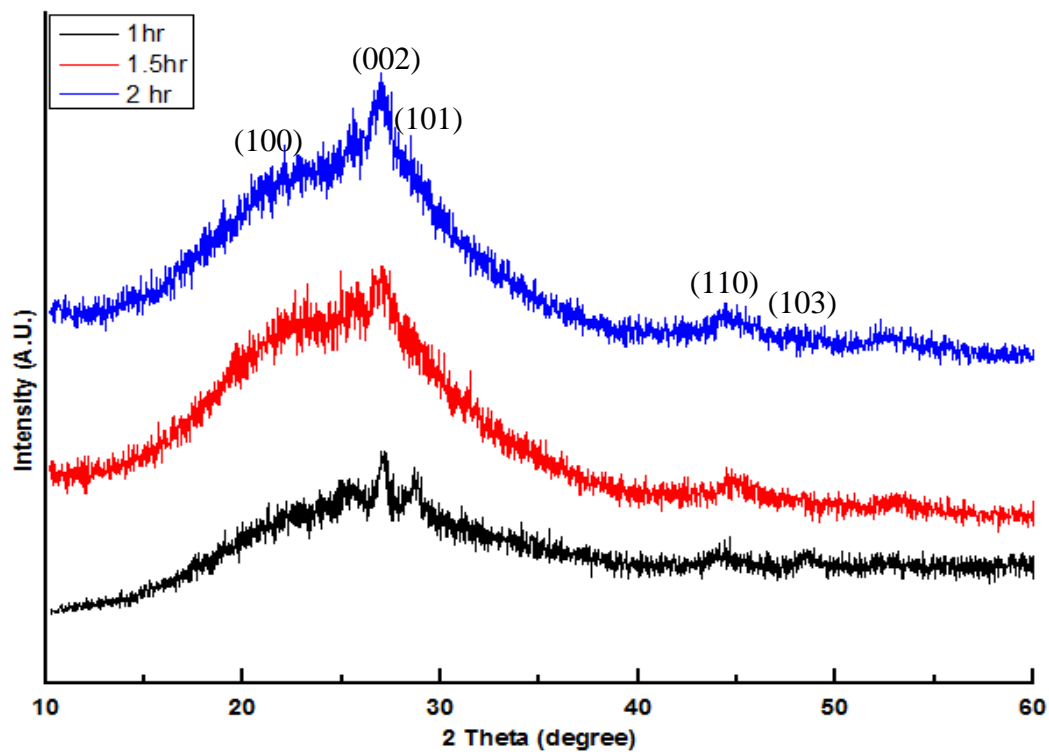
Figure 1. X-ray diffraction patterns of as deposited Cd-Zn sulphide films of different thicknesses.
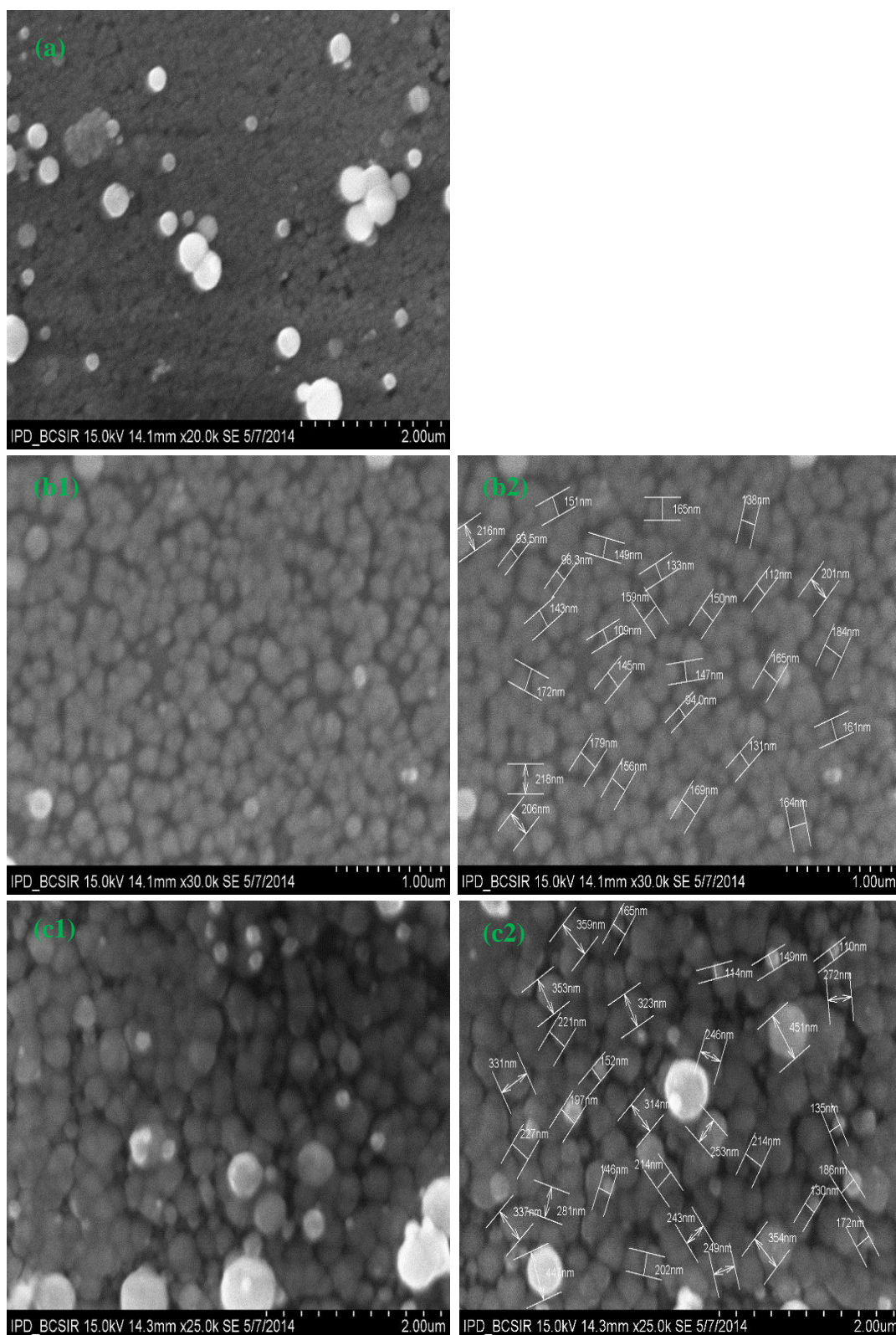
Figure 2. SEM images of Cd-Zn sulphide films deposited for (a) 1 hr, (b) 1.5 hr, and (c) 2 hr.
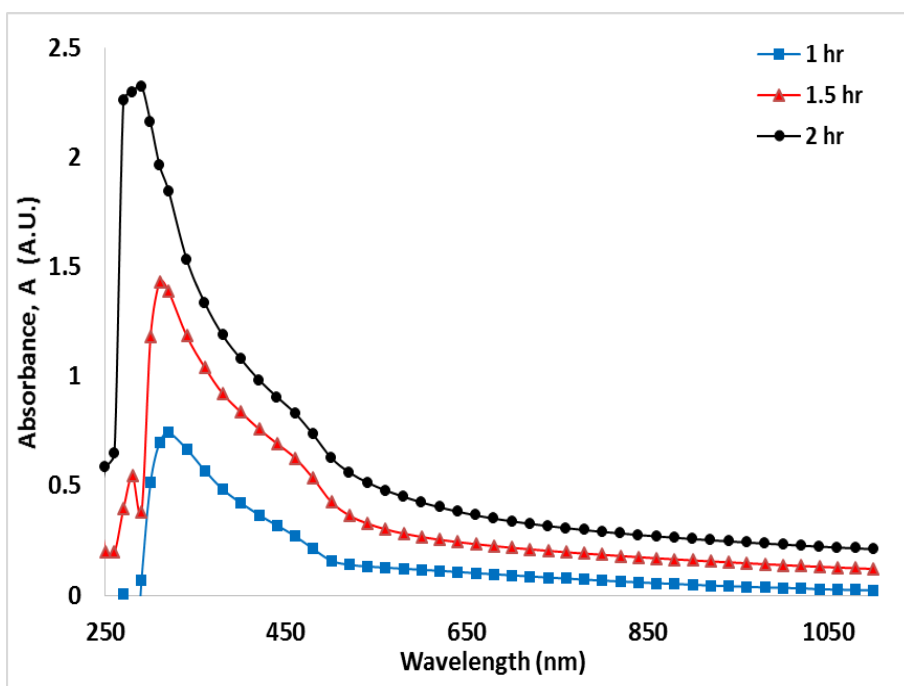
Figure 3. UV-Vis absorbance spectra of Cd-Zn sulphide films deposited for 1 hr, 1.5 hr, and 2 hr.
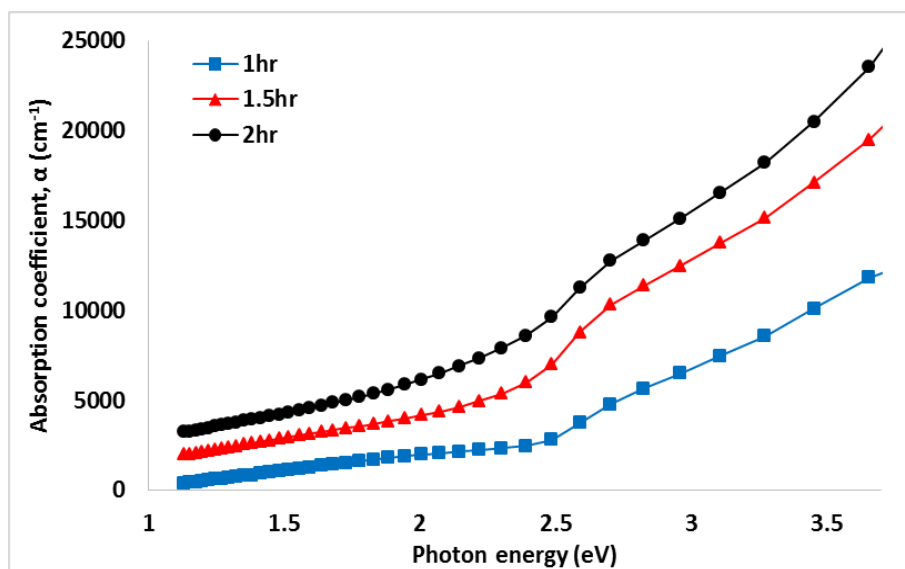
Figure 4. Absorption coefficient vs photon energy spectra of Cd-Zn sulphide films deposited for 1 hr, 1.5 hr, and 2 hr.
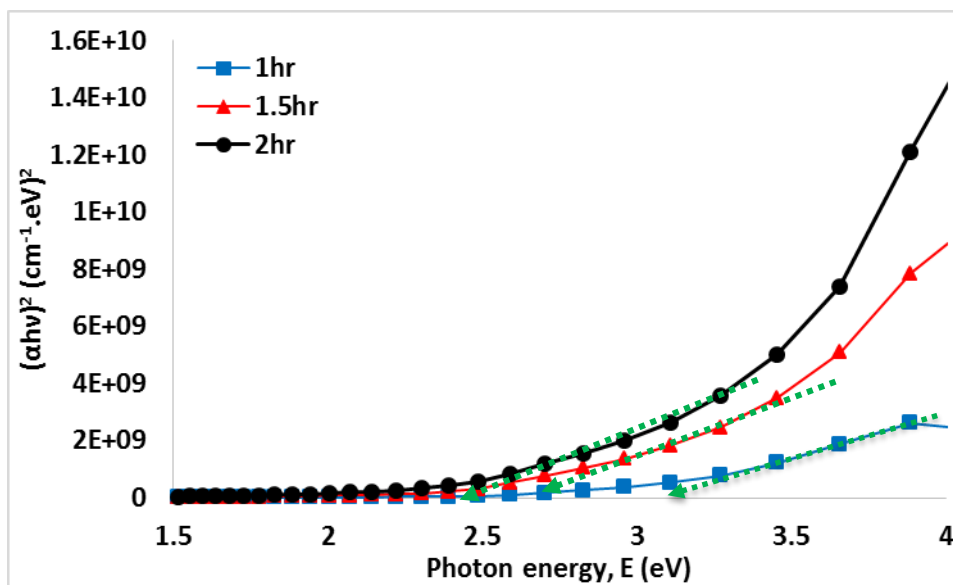
Figure 5. Tauc plots of $(\alpha h\nu)^2$ vs $h\nu$ for as deposited Cd-Zn sulphide films of different thicknesses.
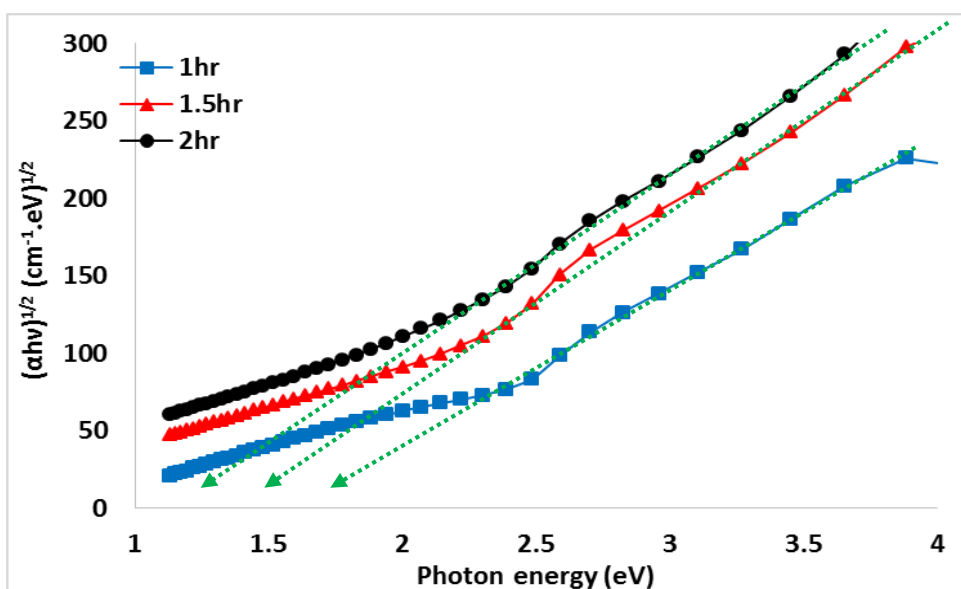
Figure 6. Tauc plots of $(\alpha h\nu)^{1/2}$ vs photon energy for as deposited Cd-Zn sulphide films of different thicknesses.
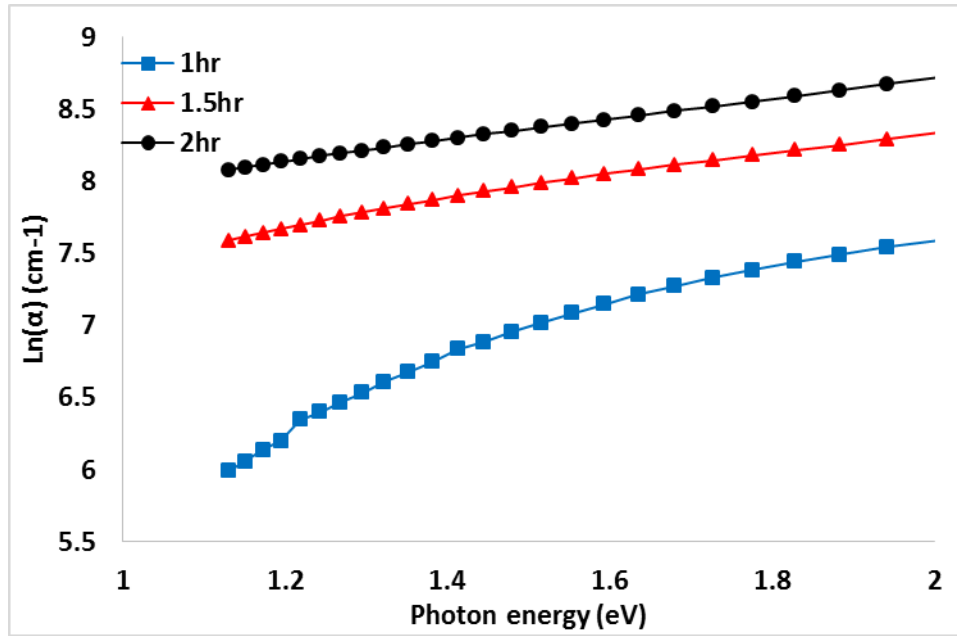
Figure 7. Urbach plots of Ln(α) vs *hv* for as deposited Cd-Zn sulphide films of different thicknesses.

Table 1. Thicknesses, crystallite size and lattice constants of the Cd-Zn sulphide films at various deposition times.

Film deposition times (hr)	Film thickness, d (nm)	Crystallite size, D (nm)	Lattice constants (nm)	
			a	c
1.0	1320	18.23	4.101	6.810
1.5	1420	15.12	4.121	6.952
2.0	1510	11.05	4.259	6.996

Table 2. Optical absorbance values of Cd-Zn sulphide thin films at various film thicknesses.

Film deposition times (hr)	Film thickness, d (nm)	Maximum optical absorbance, A (%)	Wavelength at maximum absorbance, λ (nm)
1.0	1320	74.20	320
1.5	1420	89.10	310
2.0	1510	95.40	290

Table 3. Energy band-gaps of as deposited Cd-Zn sulphide films at various film thicknesses.

Film deposition times (hr)	Film thickness, d (nm)	Direct band-gap, E_d (eV)	Indirect band-gap, E_i (eV)
1.0	1320	3.10	1.60
1.5	1420	2.65	1.30
2.0	1510	2.45	1.20

Table 4. Urbach energy and steepness parameters of Cd-Zn sulphide films at various film thicknesses.

Film deposition times (hr)	Film thickness, d (nm)	Urbach energy, E_U (eV)	Steepness parameters, σ
1.0	1320	1.25	0.020
1.5	1420	1.57	0.016
2.0	1510	1.58	0.015